Journal of Power Sources 201 (2012) 382–386

Contents lists available at SciVerse ScienceDirect

Journal of Power Sources

journal homepage: www.elsevier.com/locate/jpowsour

Short communication

Dual-template synthesis of $Co(OH)_2$ with mesoporous nanowire structure and its application in supercapacitor

Tong Xue, Xin Wang, Jong-Min Lee*

School of Chemical and Biomedical Engineering, Nanyang Technological University, Singapore 637459, Singapore

ARTICLE INFO

Article history:
Received 31 August 2011
Received in revised form 18 October 2011
Accepted 26 October 2011
Available online 18 November 2011

Keywords:
Dual templates
Porous anodic alumina templates
Lyotropic liquid crystalline templates
Mesoporous nanowires
Capacitor

ABSTRACT

A novel ordered mesoporous $Co(OH)_2$ nanowire structure has been successfully fabricated by a dual-template method utilizing porous anodic alumina (PAA) and lyotropic liquid crystal (LLC) through potentiostatic electrodeposition technique. The mesoporous ordered hexagonal structure with cylindrical channels in $Co(OH)_2$ nanowires is confirmed by low-angle X-ray diffraction (XRD) and transmission electron microscopy (TEM). A capacitance of 993 F g^{-1} for the mesoporous $Co(OH)_2$ nanowire array is obtained from charge/discharge measurement at current density of 1 A g^{-1}, indicating that the unique mesoporous nanowire structure can enhance its electrochemical properties.

1. Introduction

Electrochemical supercapacitors (ECs) are well known as attractive energy storage devices for application because of their high power energy storage ability [1]. The range of potentially practical applications of ECs extends from mobile device to electric vehicles. Based on the different nature of charge-storage mechanism, electrochemical capacitors are classified into two forms: electrochemical double layer capacitors (EDLCs) and redox capacitors (pseudocapacitors). Carbon-based materials [2,3] with high specific surface area are widely utilized as EDLCs which exhibit a nonfaradaic reaction with accumulation of charges at the electrode/electrolyte interface. Subsequently, conducting polymers [4,5] and transition metal oxides and hydroxides [6–11] have been identified as possible electrode materials for redox capacitors which utilize the charge-transfer pseudocapacitance arising from reversible faradaic reactions occurred at the electrode surface. Redox capacitors attract much more attention than EDLCs because of their better capacitive characteristics which are not only limited by specific surface area but decided by the faradaic redox character of materials themselves as well [12]. Among all the candidates of redox electrode materials, $Co(OH)_2$ has generated growing research activities and extensive studies in the field for its layered structure with large interlayer spacing, great reversibility and high specific capacitance [10,13–16]. At the beginning, precipitation methodology was used to synthesize $Co(OH)_2$ for supercapacitor, but it shows the very low specific capacitance in a range of 200–400 F g^{-1} [13,17,18]. With the development of self-assemble nanotechniques, template synthesis was paid much attention as a new kind of fabricated technology of ordered nanomaterials. One particular approach is to use porous anodic alumina (PAA) template to obtain nanowire arrays with combined lyotropic liquid crystalline (LLC) template as pore-directing agent together [19–23], which maintains the topology of the phase throughout the progress of the reaction and holds the ability to fabricate mesoporous nanowires with high surface area via electrodeposition. In this paper, we fabricated a novel mesoporous nanowire structure of $Co(OH)_2$ by confined LLC phases in cylindrical pores of PAA membranes.

2. Experimental

Porous anodic alumina (PAA) template was synthesized by anodizing Al/Ti/Si substrate in 0.3 mol L^{-1} oxalic acid solution at 40 V and 4 °C for 4 h. Lyotropic liquid crystalline (LLC) template was prepared from mixing 50 wt% Brij56 (polyoxyethylene(10) cetyl ether, C_{16} $[EO]_{10}$) and 50 wt% Co^{2+} electrolyte (1.2 M $Co(NO_3)_2$ and 0.075 M $NaNO_3$) to achieve homogeneous mixtures. The electrochemical deposition [24–26] was conducted on an electrochemical workstation (CHI660d, CH Instruments Inc., Shanghai), by using a conventional three-electrode system composed of a 0.6 cm^2 PAA/Ti/Si working electrode, a large surface area platinum counter electrode, and a standard Ag/AgCl electrode. After electrodeposition, the electrode was immersed into ethanol to remove Brij56

* Corresponding author. Tel.: +65 6513 8129; fax: +65 6794 7553.
E-mail address: jmlee@ntu.edu.sg (J.-M. Lee).

0378-7753/$ – see front matter © 2011 Elsevier B.V. All rights reserved.
doi:10.1016/j.jpowsour.2011.10.138

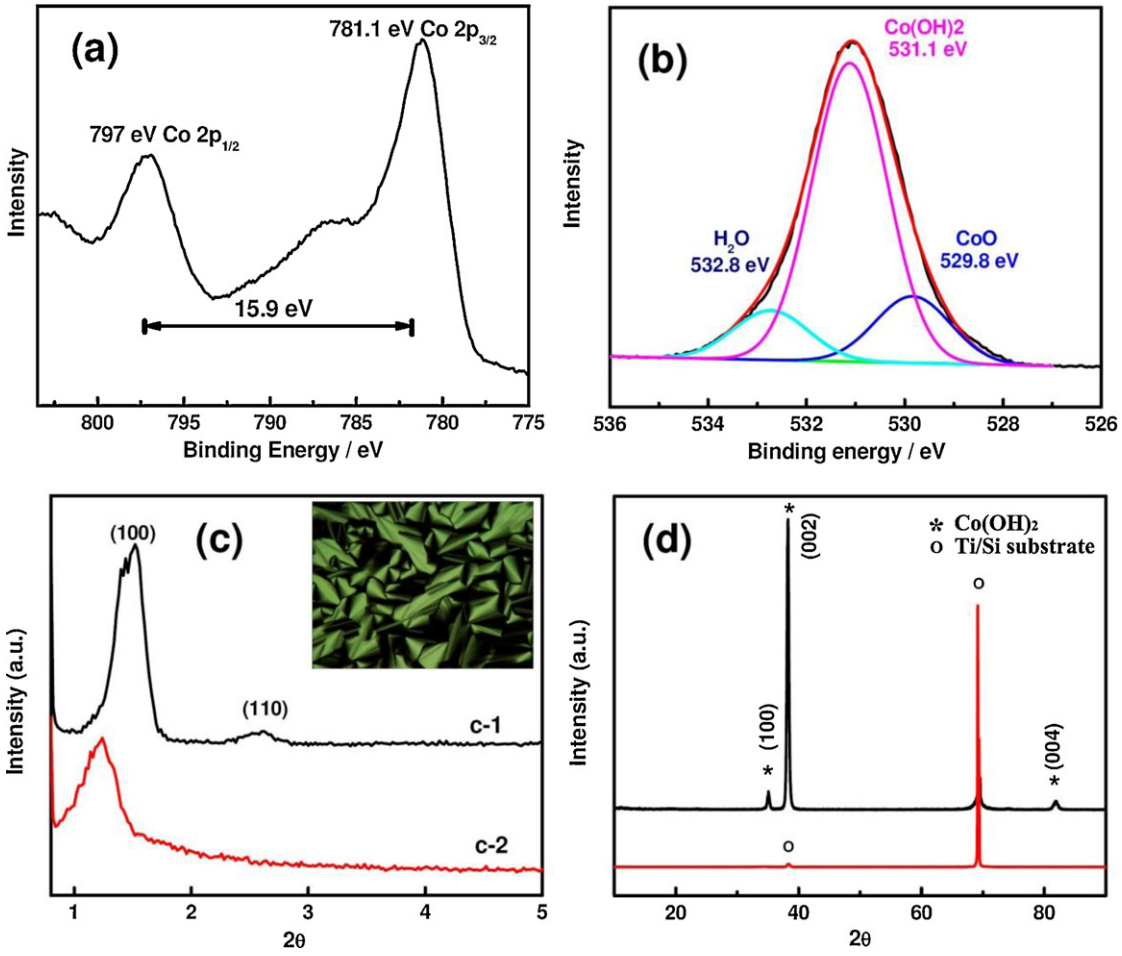

Fig. 1. XPS Co $2p_{1/2}$, Co $2p_{3/2}$ spectra (a) and O 1s spectra (b) of electrodeposited mesoporous $Co(OH)_2$ nanowires. Low-angle XRD patterns of Co^{2+} liquid crystalline phase (c-1) and mesoporous $Co(OH)_2$ nanowires (c-2) (upper right is POM image of hexagonal structure.). Wide-angle XRD patterns of mesoporous $Co(OH)_2$ nanowires (d).

for 2 h and ethanol was replaced at least 3 times until the surfactant was removed entirely. PAA template was removed by using 1 M NaOH. Finally, the electrode was rinsed by ultrapure water and dried in ambient atmosphere.

X-ray photoelectron spectroscopy (XPS) was performed on a Kratos AXIS Ultra HAS spectrometer equipped with a monochromatized Al Kα X-ray source to study the chemical state of electrodeposited $Co(OH)_2$ film. The LLC phase structure was investigated by polarized optical microscopy (POM, XJP400T, KOZO) equipped with a KER-3100-08S heating stage and temperature control unit. Low angle X-ray diffraction (XRD) patterns were recorded on a Bruker D8 Advance diffractometer with Cu-Kα as the radiation source ($\lambda = 0.154$ nm). Field emission scanning electron microscopy (FESEM) was carried out with a JEOL-JSM-6700F microscope operated at 5 kV for morphology of PAA template and $Co(OH)_2$ nanowires on the substrate. Transmission electron microscopy (TEM) was carried out with JEOL-2010 microscopes operated at 300 kV. The electrochemical measurements of the samples were performed on CHI660d electrochemical workstation.

3. Result and discussion

$Co(OH)_2$ synthesis is carried out using potentiostatic electrodeposition method at constant cathodic potential in the range of −0.6 to −1.0 V. The mechanism of $Co(OH)_2$ electrodeposition is proposed to be as follows:

$$NO_3^- + 7H_2O + 8e^- \Rightarrow NH_4^+ + 10OH^- \quad (1)$$

$$Co^{2+} + 2OH^- \Rightarrow Co(OH)_2 \quad (2)$$

XPS was employed to examine the chemical state of deposited $Co(OH)_2$ nanowires. Fig. 1 shows the Co 2p (a) and O 1s (b) spectra of XPS deposit. As shown in Fig. 1a, there are two main Co 2p spectrums which locate at binding energy 797 eV (Co $2p_{1/2}$) and 781.1 eV (Co $2p_{3/2}$) with satellite peaks due to plasmon losses and final state effects respectively. The distance between these two peaks ($\Delta E_b = 15.9$ eV) indicates Co existed as $Co(OH)_2$ version [16,27]. Fig. 1b shows the XPS spectra and curve fitting results of O 1s. Inside, the middle strongest spectrum indicates the existing of $Co(OH)_2$ (531.1 eV) which is the dominating form within the deposit. The figure also shows two smaller shoulder spectrums, in which the right one can be assigned as CoO (529.8 eV) attributed to a small degree of dehydroxylation upon drying and the left one can be ascribed to structural water (532.8 eV) [28]. The crystalline structure of $Co(OH)_2$ was further confirmed by wide-angle XRD as shown in Fig. 1d. The three main peaks with indexes of (1 0 0), (0 0 2) and (0 0 4) can be assigned to the diffraction of layered α-$Co(OH)_2$ [10,15] (JCPDS No. 74-1057) except one peak labeled as Ti/Si substrate. Fig. 1c (upper right) shows the POM photo of $Co(NO_3)_2$ LLC phase. Its focal conic fan texture indicates the phase exists as the hexagonal form. The low-angle XRD patterns of the template mixture (Fig. 1c-1) display two well-resolved peaks with d-spacing of 58.1 and 33.7 Å at 2θ equal to 1.52° and 2.62°, respectively, which can be indexed as the (1 0 0) and (1 1 0) planes of the P6 mm space group (hexagonal structure) for reciprocal ratio of d are $1:\sqrt{3}$. The pore to pore distance of this hexagonal LLC template, calculated

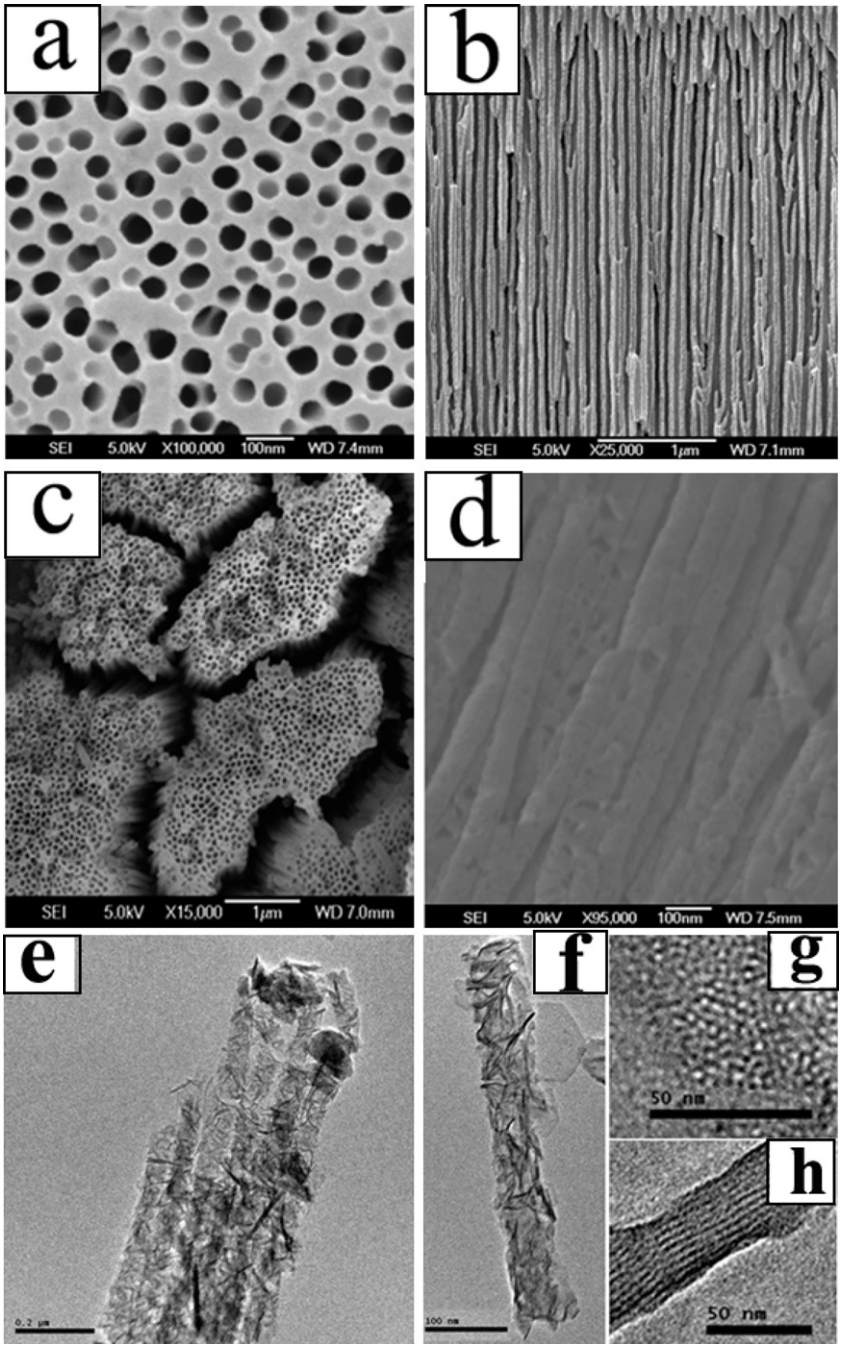

Fig. 2. SEM images of PAA templates (end view (a) and cross view (b)) and mesoporous $Co(OH)_2$ nanowire (end view (c) and side view (d)). TEM images of mesoporous $Co(OH)_2$ nanowires (e and f). (g) and (h) are the end view and side view of the pores respectively.

by $d_{100}/\cos 30$, is 6.7 nm. Meanwhile, the resulting mesoporous $Co(OH)_2$ nanowire also shows a strong reflection peak at 2θ equals to 1.24°. The peak is also assigned to d_{100} plane of the P6mm space group with d-spacing of 71.2 Å and pore to pore distance of 8.2 nm. This result suggests that the liquid crystalline structures were still retained after the electrosynthesis. The presence of diffraction peak indicates that the ordered mesophase structure in the template is preserved in the deposited film.

The surface morphologies of PAA template and porous $Co(OH)_2$ nanowire were examined by FESEM as shown in Fig. 2. From surface (Fig. 2a) and side (Fig. 2b) images of PAA template, the pore diameter of templates was found to be around 50–65 nm with fine channels. As shown in Fig. 2c and d, after removing the PAA template, the diameter of templated $Co(OH)_2$ nanowires still kept as 65 nm, which means the fully duplicated procedure was processed. The rough wall of nanowires indicates pores existing and a few structural defects. The wires are inclined to agglutinate each other with holly structure at topside. It can be explained by nanosheet-like morphology of $Co(OH)_2$ films reported from Zhou et al. [10]. The growth of nanowires still obeys the rules of sheet packing. This loose packed structure causes weak holding strength between nanowires and substrate, and then leads to wires aggregation.

The sheet packed structure was further confirmed by TEM as shown in Fig. 2. Fig. 2e and f shows the nanowire structures of $Co(OH)_2$ at different magnifications. As expected, the ordered

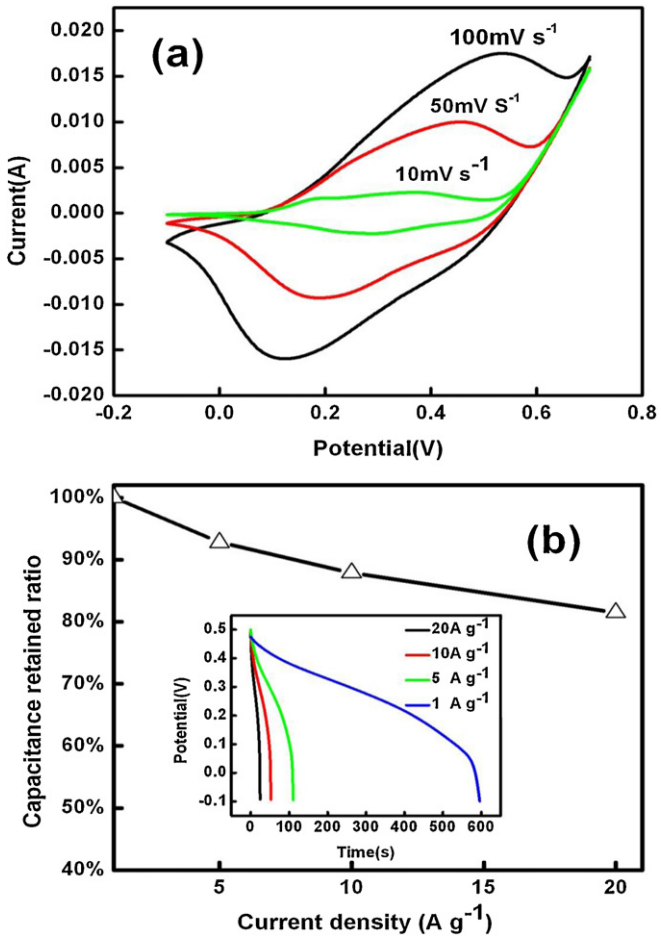

Fig. 3. Electrochemical properties of ordered mesoporous $Co(OH)_2$ nanowire electrode: (a) CV curves at different scan rates and (b) discharge curves at different current densities in potential range of −0.1 V to 0.5 V vs. Ag/AgCl.

porous morphologies on the nanosheets of $Co(OH)_2$ wires were observed by TEM shown in Fig. 2g and h. The light regions correspond to pores left after removal of the surfactant template from the electrodeposited wires and the dark areas represent the electrodeposited $Co(OH)_2$. The uniform and well-ordered hexagonal pores with cylindrical channels of about 3.6 nm in diameter were observed. The pore to pore distance is around 7.9 nm and the pore wall thickness is about 4.3 nm, which are consistent with 100 peak appeared in the low-angle XRD patterns.

Both cyclic voltammetry (CV) curve and chronopotential charge–discharge methods were used to investigate capacitor behavior of the materials. For both electrochemical measurements of $Co(OH)_2$, 1 M KOH aqueous solution was used as electrolyte. In this electrochemical system, two reversible redox reactions can occur during potential sweep of synthesized $Co(OH)_2$ electrode. The reactions can be expressed as follows [29]:

$$Co(OH)_2 + OH^- \leftrightarrow CoOOH + H_2O + e^- \quad (3)$$

$$CoOOH + OH^- \leftrightarrow CoO_2 + H_2O + e^- \quad (4)$$

As shown in Fig. 3a, the CV curves of mesoporous $Co(OH)_2$ nanowires measured at scan rates of 100, 50 and 10 mV s^{-1} were displayed respectively. One pair of redox peaks can be observed from the cycles at scan rate of 100 and 50 mV s^{-1}, indicating that the mechanism of capacitance generation is based on redox capacitor because of electron-transfer process which is distinct from an ideal rectangular shape produced by electric double-layer capacitors. During the electron transfer procedure, only one oxidation peak, appeared at around 0.4 V, possibly due to the production of CoOOH as an intermediate form which just existed for quite short time and then converted into CoO_2 rapidly. The actual reversible reaction at scan rate of 100 and 50 mV s^{-1} can be written as follows:

$$CoOOH + OH^- \leftrightarrow CoO_2 + H_2O + e^- \quad (5)$$

At scan rate decreasing to 10 mV s^{-1}, two oxidation peaks appear, proving that $Co(OH)_2$ has enough time to remain in CoOOH form which can be changed into CoO_2.

Fig. 3b shows the discharge curves of the ordered mesoporous H_I–$Co(OH)_2$ nanowire array electrode measured at different discharge current densities within potential window of −0.1 to 0.5 V. The specific capacitance values were calculated to be 993, 922, 873 and 810 F g^{-1} corresponding to the discharging current densities of 1, 5, 10 and 20 A g^{-1}, respectively. The highest capacitance of 993 F g^{-1} was obtained at discharge current density of 1 A g^{-1}. $Co(OH)_2$ mesoporous nanowire array has a slightly lower capacitance than mesoporous film [10], possibly due to the collapse of the end parts of nanowires under different synthesis conditions (e.g. electrodeposition potential, drying method and electrode working area) [30]. Further work is needed to solve the problems and enhance its performance. Fig. 3b also summarized the capacitance retained ratios of the electrodes prepared in this study as a function of current density. Using capacitance obtained at 1 A g^{-1} as 100% retention, when the current density was increased from 1 to 20 A g^{-1}, the capacitance of mesoporous $Co(OH)_2$ nanowire array electrodes reserved 100%, 92.8%, 87.9% and 81.5%, respectively, indicating that the capacitance of the $Co(OH)_2$ wires is not significantly influenced with increasing of the current density. From the results, mesoporous nanowires obtained from the dual templates behave excellent performance which can be attributed to the high porosity and well dispersion of $Co(OH)_2$. These structural factors increase ionic transport, shorten electron traveling distance and reduce interface resistance.

4. Conclusion

In summary, we have demonstrated a novel approach for electrosynthesis of mesoporous $Co(OH)_2$ nanowire array electrode via PAA templates with Brij56 LLC templates as pore-generated agent. The results of TEM and low angle XRD indicate the presence of ordered porous nanostructures and supported a direct templating mechanism for the electrodeposition of mesoporous $Co(OH)_2$ wires. The electrochemical results show the attractive specific capacitance of 993 F g^{-1} at current density of 1 A g^{-1} which has potential application to be used as electrode material in supercapacitors.

Acknowledgement

This work is supported by Startup Grant of Nanyang Technological University and Academic Research Fund (RG21/09) of Ministry of Education in Singapore.

References

[1] B.E. Conway (Ed.), Electrochemical supercapacitors, Kluwer Academic Publishers, New York, 1999.
[2] E. Frackowiak, F. Béguin, Carbon 39 (2001) 937–950.
[3] C. Lin, B.N. Popov, H.J. Ploehn, Journal of The Electrochemical Society 149 (2002) A167–A175.
[4] A. Rudge, J. Davey, I. Raistrick, S. Gottesfeld, J.P. Ferraris, Journal of Power Sources 47 (1994) 89–107.
[5] A. Rudge, I. Raistrick, S. Gottesfeld, J.P. Ferraris, Electrochimica Acta 39 (1994) 273–287.
[6] J.P. Zheng, P.J. Cygan, T.R. Jow, Journal of The Electrochemical Society 142 (1995) 2699–2703.
[7] A.A.F. Grupioni, E. Arashiro, T.A.F. Lassali, Electrochimica Acta 48 (2002) 407–418.

[8] C. Lin, J.A. Ritter, B.N. Popov, Journal of The Electrochemical Society 145 (1998) 4097–4103.
[9] V. Srinivasan, J.W. Weidner, Journal of The Electrochemical Society 147 (2000) 880–885.
[10] W.-j. Zhou, J. Zhang, T. Xue, D.-d. Zhao, H. -l. Li, Journal of Materials Chemistry 18 (2008) 905–910.
[11] Zhao, Zhou, Li, Chemistry of Materials 19 (2007) 3882–3891.
[12] B.E. Conway, Journal of The Electrochemical Society 138 (1991) 1539–1548.
[13] Z. Hu, L. Mo, X. Feng, J. Shi, Y. Wang, Y. Xie, Materials Chemistry and Physics 114 (2009) 53–57.
[14] T. Zhao, H. Jiang, J. Ma, Journal of Power Sources 196 (2011) 860–864.
[15] V. Gupta, T. Kusahara, H. Toyama, S. Gupta, N. Miura, Electrochemistry Communications 9 (2007) 2315–2319.
[16] J.-K. Chang, C.-M. Wu, I.W. Sun, Journal of Materials Chemistry 20 (2010) 3729–3735.
[17] E. Hosono, S. Fujihara, I. Honma, M. Ichihara, H. Zhou, Journal of Power Sources 158 (2006) 779–783.
[18] C. Yuan, X. Zhang, B. Gao, J. Li, Materials Chemistry and Physics 101 (2007) 148–152.
[19] S. Baber, et al., Nanotechnology 21 (2010) 165603.
[20] A. Takai, T. Saida, W. Sugimoto, L. Wang, Y. Yamauchi, K. Kuroda, Chemistry of Materials 21 (2009) 3414–3423.
[21] A. Foyet, A. Hauser, W. Schäfer, Journal of Solid State Electrochemistry 12 (2008) 47–55.
[22] Y. Zhong, C.-L. Xu, L.-B. Kong, H.-L. Li, Applied Surface Science 255 (2008) 3388–3393.
[23] C. Xu, Y. Zhao, G. Yang, F. Li, H. Li, Chemical Communications (2009) 7575–7577.
[24] J.-M. Lee, H. Dyar, J.E. Taylor, R. Carpio, Journal of Electrochemical Society 153 (2006) C265–C271.
[25] Y. Cao, J.-M. Lee, A.C. West, Plating and Surface Finishing 90 (2003) 40–45.
[26] J.-M. Lee, A.C. West, Journal of Electrochemical Society 152 (2005) C645–C651.
[27] L. Li, H. Qian, J. Ren, Chemical Communications (2005) 4083–4085.
[28] R. Xu, H.C. Zeng, Chemistry of Materials 15 (2003) 2040–2048.
[29] L. Cao, F. Xu, Y.Y. Liang, H.L. Li, Advanced Materials 16 (2004) 1853–1857.
[30] J.-M. Lee, Electrochimica Acta 51 (2006) 3256–3260.